Check for updates

Received: 28 February 2022 | Revised: 11 April 2022 | Accepted: 18 May 2022

DOI: 10.1002/poc.4386

RESEARCH ARTICLE

Journal of Physical Organic Chemistry WILEY

The optical spectra of DMAC-based molecules for organic light-emitting diodes: Hybrid-exchange density functional theory study

Yuting Wang | **Wei Wu** | **Kwang Leong Choy**

UCL Institute for Materials Discovery, University College London, London, UK

Correspondence
Wei Wu and Kwang Leong Choy, UCL Institute for Materials Discovery, University College London, Malet Place, WC1E 7JE, London, UK.
Email: wei.wu@ucl.ac.uk and k.choy@ucl.ac.uk

Funding information
European Research Council, Grant/Award Number: 545083

Abstract

Organic light-emitting diodes (OLED) have considerable advantages over the conventional counterpart. Molecular design by simulations is important for the discovery of new material candidate to improve the performance of OLED. Recently, thermally assisted delayed fluorescence OLED based on DMAC (9,9-dimethyl-9,10-dihydroacridine)-related molecules have been found to have superior performance. In this work, a series of first-principles calculations are performed on DMAC-DPS (diphenylsulfone, emission of blue-color light), DMAC-BP (benzophenone, green), DMAC-DCPP (dicyclohexylphosphonium, red), and the newly designed DMAC-BF (enaminone difluoroboron complexes, red) molecules, based on time-dependent density-functional theory, the hybrid-exchange density functional, and the long-range corrected hybrid-exchange density functional. By varying the percentage of Hartree–Fock (HF) exchange in the hybrid-exchange functional, the emission spectra can be over 97% fitted to the experimental results. We found that the fitted proportion of HF will increase as the wavelengths of the molecules decrease (30% for DPS, 20% for BP, and 10% for DCPP). By contrast, the long-range corrected hybrid-exchange density functional can lead to a good estimate on the absorption spectra. In addition, we have also applied our fitting computational procedure to the newly designed molecule. The molecular orbitals involved in the related excited states have also been investigated for these molecules, which show a common charge-transfer characteristic between the acceptor part (DPS/BP/DCPP/BF) and the donor (DMAC).

KEYWORDS

density functional theory, emission spectra, light-emitting molecules, organic light-emitting diode, thermally activated delayed fluorescence

This is an open access article under the terms of the Creative Commons Attribution-NonCommercial License, which permits use, distribution and reproduction in any medium, provided the original work is properly cited and is not used for commercial purposes.
© 2022 The Authors. *Journal of Physical Organic Chemistry* published by John Wiley & Sons Ltd.

1 | INTRODUCTION

With the development of the information technology and electronics, the electronic display screens carrying a vast amount of information have occupied every corner of people's lives in recent years.[1] The requirements for the better performance of the electronic devices for information technologies are also becoming higher.[2] The traditional display technologies, including cathode ray tube (CRT) and liquid crystal displays (LCD), have gradually failed to meet people's demands for the high responsiveness, portability, and flexibility. Organic light-emitting diode (OLED), as an emerging display technology, has shown many advantages, such as low driving voltage, fast response speed, high luminous brightness, lightweight, and strong flexibility.[3] It is highly expected that OLED will become the next generation of devices for modern ultrathin and large-area electronic displays.[3,4] The light-emitting material, the cornerstone for OLED devices, has become one of the most important research topics in this field. The light-emitting devices designed in the early development stage for OLED only exploited the singlet excitons in the luminescent material to emit fluorescence, and the internal quantum efficiency would go up to 25%, due to the limited access to the other spin states of the electron–hole pair (1/4 for singlet and ¾ triplet).[5] In the later development, by doping phosphorescent dyes (PtOEP, 2,3,7,8,12,13,17,18-octaethyl-21H,23H-porphine platinum(II)) in the light-emitting layer material, the first organic electro-phosphorescent device was fabricated,[6] which can use both the singlet (S_1) and the triplet (T_1) excitons to emit light and the singlet can relax to the triplet through intersystem crossing (ISC), achieving ultrahigh quantum efficiency. However, the high cost of phosphorescent materials has hindered the large-scale commercialization.

Thermally activated delayed fluorescent (TADF) materials entirely composed of organic materials were discovered in 2012, with high exciton utilization rate and internal and external quantum efficiency (EQE).[7] In principles, the energy difference between the T_1 and S_1 in TADF materials can be very small during excitation. Thus, triplet excitons can transform to singlet through reverse ISC (RISC) mechanism, leading to a high exciton utilization rate and fluorescent efficiency. Recently, the inverted singlet–triplet gap (the excited singlet state is lower than the triplet) has attracted much attention because this can lead to more efficient conversion from the triplet to the singlet.[8] Thus far, many TADF molecules have been synthesized to have high luminous efficiency.[9] For example, DMAC (9,9-dimethyl-9,10-dihydroacridine)-TRZ (2,4,6-triphenyl-1,3,5-triazine) molecules have been reported to achieve an EQE of 26.5% with a sky-blue emission (the wavelength ~490 nm).[10] OLED devices made of TspiroS (acridine-9,9′-anthracene-10′,9″-thioxanthene)-TRZ and TDBA-DI (5-(2,12-di-tert-butyl-5,9-dioxa-13b-boranaphtho[3,2,1-de]anthracen-7-yl)-10,15-diphenyl-10,15-dihydro-5H-diindolo[3,2-a:3′,2′-c]carbazole) molecules have also been reported to have an EQE of over 30%.[11,12] However, the TADF molecules still have some drawbacks such as relatively broad emission spectra and impure colors, which limits its further application.[13]

In order to find suitable molecular design methods and improve the luminescence performance of TADF materials, the cutting-edge density functional theory (DFT) calculations can be utilized to analyze and predict the properties of molecules and provide a reference or guidance for experimental research.[14–16] The theoretical studies of OLED molecules can provide important information about the geometric structure and electronic properties of molecules. Through comparing with experimental results, modeling and calculation results can help researchers to gain knowledge about the relationship between molecular structure, electronic properties, and optical properties, bringing guidance for future molecular designs. DFT method has previously been used to theoretically calculate the excited states and predict the absorption and emission spectra of the molecules, which could provide important clues to improve the optical properties of TADF molecules.[14,17,18] The method of varying the Hartree–Fock (HF) exchange proportion in the DFT calculations has been applied to the calculations of the vertical absorption energies for TADF molecules.[17,18] This methodology can be further extended to the calculations of the singlet–triplet splitting and the emission spectra as well. The theoretical and experimental work on TADF molecules, including those based on DMAC molecules, has been carefully reviewed.[14] Especially, the quantification of the size of the singlet–triplet splitting through DFT and time-dependent DFT (TDDFT) with the optimal HF percentages and long-range corrections has been discussed in detail.

Recently, DMAC (9,9-dimethyl-9,10-dihydroacridine)-DPS (diphenylsulfone), DMAC-BP (benzophenone), DMAC-DCPP (dicyclohexylphosphonium), and DMAC-BF (enaminone difluoroboron complexes) have been studied experimentally for blue, green, and red colors (DCPP and BF), respectively.[19–22] Here, DMAC works as a donor, whereas the other molecular moieties (DPS, BP, DCPP, and BF) work as acceptors with different colors of light. Especially the discovery of the DMAC-based molecules is inspiring for the design of molecules to enhance the performance of TADF molecules. The DMAC-DPS molecules have been designed and

synthesized previously,[19] in combination with the DFT modeling based on hybrid-exchange density functional, which is very successful. The authors therein have synthesized the DMAC-DPS molecule with blue color and identified six potential candidates with a small singlet–triplet splitting. The EQE can be achieved up to 19.5%, comparable with the phosphorescence molecules.[19] This work has laid the foundation for the follow-up DMAC-related molecules for OLED, thus opening up a new avenue for the OLED materials research. Moreover, Jiang et al. have recently synthesized the DMAC-BP[20] (green color) with an EQE of 8.1%, in which the author emphasized that DMAC-BP is highly efficient, is low cost, and does not need extra doping. This is also further confirmed by the very small singlet–triplet splitting (<0.10 eV) of the DMAC-BP molecule obtained from theoretical calculations.[23] Wang et al.[21] have found the DMAC-DCPP molecule has a high EQE of 10.1%, in which the molecular connection modes have also been investigated. Theoretical calculations for the DMAC-DCPP molecule show that it has a very small singlet–triplet energy difference, which is beneficial for the TADF process. However, the calculated oscillator strength of the molecule is extremely small, which could be due to the rotational relaxation between the donor and the acceptor moieties.[21] In the experimental studies, a single DMAC molecule has been combined with a single BF molecule to fabricate the red-color TADF OLED materials.[22] Although a significant progress has been made for the DMAC-based TADF molecules, they still suffer from the lack of sharp emission line for the red color, which could be solved by using theoretical design of molecule structures based on DFT. Recently, this methodology has been applied to study the potential of charge-transfer molecules for the application of greenhouse-integrated organic solar cells.[24–28] In addition, machine learning can also be used in organic electronics to screen the potential molecular candidates for a specific purpose, such as the optimal optical spectra.[29] It has been shown that increasing the number of donors in molecular design can enhance the electron-donating ability, which would facilitate the reduction of singlet–triplet state energy difference and thus improves the performance of TADF molecules.[30] Therefore, based on this idea, here, we include two DMAC molecules, that is, the DMAC-BF molecule, in the molecular design to observe the variation of the emission spectra. A table summarizing the properties of the DMAC-based TADF molecules is shown below (Table 1).

In this paper, we used TD-DFT methods to calculate the properties of three TADF molecules based on DMAC donors (DMAC-DPS, DMAC-BP, and DMAC-DCPP) and compared the calculation results with the experimental ones in the literature. Through modifying the proportion of the HF exchange in the hybrid functionals, the calculation results fit the experimentally observed emission spectra well. We have also carried out the DFT and TD-DFT calculations with long-range corrections.[31] Based on the above experimental results, we designed a new TADF molecule, called DMAC-BF, with two DMAC donors, which is proved to possess a longer wavelength of red-light emission by our theoretical calculations. Our calculation results not only include the absorption spectra but also the emission spectra and singlet–triplet splittings for a set of typical DMAC-based TADF molecules. In our calculations, we have found that changing the HF percentage is insufficient to have a universal interpretation for the optical spectra for all the molecules considered, thus requiring further improvement on the exchange-correlation functionals. As shown in Figure 1, we have first performed the geometry optimization calculation for the singlet ground state of the molecules, followed by the excited-state geometry optimization calculations to work out the emission spectra. After the singlet ground-state geometry optimization, we can also obtain structural features, the gaps between the highest occupied molecular orbital (HOMO) and the lowest unoccupied molecular orbital (LUMO), and absorption spectra. We have computed the singlet–triplet gap after the triplet geometry optimization.

TABLE 1 A summary for the DMAC-based TADF molecules

Acceptor	EQE	Emission wavelength (nm)	Absorption wavelength (nm)	Singlet–triplet splitting (eV)
DPS[19]	19.5%	460	370	~0.08
DCPP[21]	10.1%	624	464	0.04
BP[20,23]	8.1%	520	320	0.07
BF[22]	11.3%	620	370	0.17
TRZ[10,44]	26.5%	490	300	0–0.6[a]

Note: Notice that here we show the wavelengths of the most significant emission and absorption spectra peaks.
[a]This value depends on the dihedral angle between donor and acceptor.

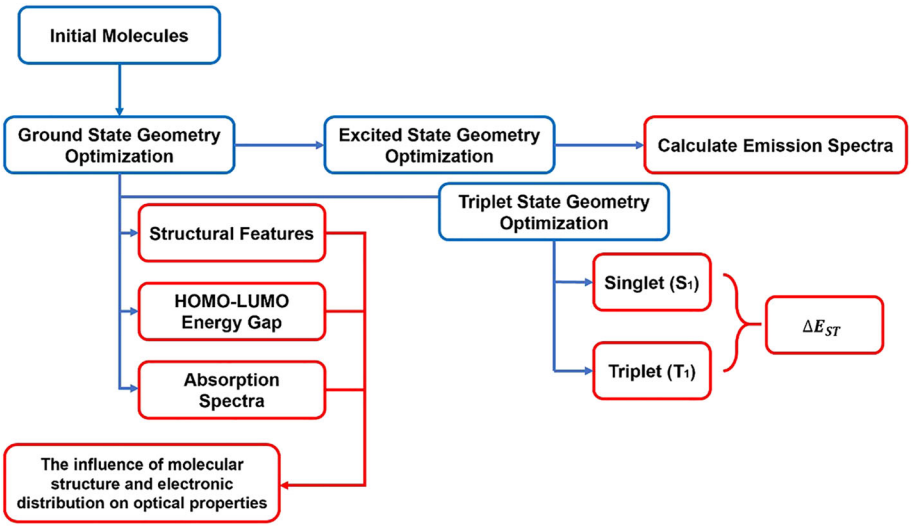

FIGURE 1 A flowchart to illustrate our computational procedures. We first performed the singlet ground-state geometry optimization to work out the absorption spectra, and then the triplet optimization to compute the singlet–triplet splitting. Finally, we have done the singlet excited-state geometry optimization to find the emission spectra

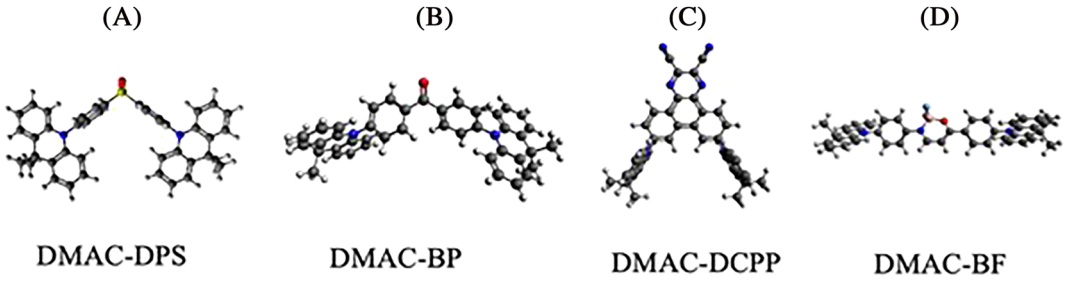

FIGURE 2 The molecular structures for TADF are shown for DMAC-DPS (A), DMAC-BP, DMAC-DCPP (C), and DMAC-BF (2 DMAC molecules) (D). H atom is in white, C in gray, N in blue, S in yellow, and O in red

2 | COMPUTATIONAL DETAILS

DFT and TD-DFT[32,33] have been used to compute the electronic structures of the chosen molecules, whose structures are shown in Figure 2. The DMAC moieties are normally on the two sides of the molecule while the acceptor moiety is in the middle. The hybrid-exchange density functionals related to B3LYP has been used for all the calculations, for which we have also modified the proportion of HF exchange in the hybrid-exchange functional (20% is for B3LYP) to match the experimental emission spectra. Recently, the long-range corrected functionals[34,35] have been used to compute the electronic structure of organic molecules. By contrast, it is more convenient to change the proportion of HF exchange based on B3LYP functional[36]; the keywords for varying the HF proportion include IOp(3/76), IOp (3/77), and IOp(3/78). We have also employed the long-range-corrected hybrid-exchange density functional CAM-B3LYP (CB) to perform both the DFT and TD-DFT calculations for a comparison.[31,34,35] The 6-31+G* basis set, including polarization and diffusion Gaussian basis functions, have been chosen for all the calculations. Gaussian 09 code[37] is used for computing the ground and excited states for the chose molecules. We have optimized the singlet ground-state and excited-state geometries to compute the absorption and emission spectra, respectively. The singlet–triplet gaps were computed at the optimized triplet state[38] because the triplet state is more relevant for the conversion between triplet and singlet excited states. In addition, we have neglected the medium effect and the dispersion force at the moment, which could lead to further studies for this type of molecules. The molecular structure and orbitals are visualized in Avogadro.[39]

3 | RESULTS AND DISCUSSION

As shown in Tables 2–4, we have compared all the relevant wavelengths and energies for DMAC-DPS, DMAC-BP, and DMAC-DCPP, respectively. The absorption wavelength here is chosen to be from the lowest optically active excited state under the singlet ground-state optimized geometry, whereas the emission spectra is from the lowest optical accessible excited state for the excited-

TABLE 2 Calculation results of DMAC-DPS (CB = CAM-B3LYP)

	λ_{abs} (nm)	λ_{em} (nm)	S_1 energy (eV)	T_1 energy (eV)	ΔE_{ST} (eV)	HOMO/LUMO (eV)
20%HF	448.79	373.63 (3rd)	3.37	2.84	0.53	−5.12/−1.75
25%HF	410.84	343.31(3rd)	3.66	3.01	0.65	−5.71/−1.91
30%HF	378.41	452.61 (1st)	3.01	2.71	0.30	−6.30/−2.07
35%HF	350.35	416.10 (1st)	3.22	2.77	0.45	−6.91/−2.24
CB	329.20	334.07 (1st)	3.26	2.65	0.59	−6.43/−0.49
Experimental emission wavelength: 460 nm						

TABLE 3 Calculation results of DMAC-BP

	λ_{abs} (nm)	λ_{em} (nm)	S_1 energy (eV)	T_1 energy (eV)	ΔE_{ST} (eV)	HOMO/LUMO (eV)
20%HF	519.65	527.27 (2nd)	2.38	2.72	−0.34	−5.02/−2.11
25%HF	474.68	480.48 (2nd)	2.60	2.85	−0.25	−5.61/−2.32
30%HF	436.66	323.39 (3rd)	2.84	2.98	−0.14	−6.21/−2.55
35%HF	404.12	311.17 (3rd)	3.98	3.21	0.77	−6.83/−2.77
CB	346.64	345.99 (2nd)	3.54	3.13	0.41	−6.33/−0.84
Experimental emission wavelength: 520 nm						

TABLE 4 Calculation results of DMAC-DCPP

	λ_{abs} (nm)	λ_{em} (nm)	S_1 energy (eV)	T_1 energy (eV)	ΔE_{ST} (eV)	HOMO/LUMO (eV)
10%HF	1100.67	611.04 (5th)	1.73	0.98	−0.75	−4.06/−2.74
15%HF	890.51	538.63 (5th)	2.39	1.91	0.48	−4.63/−2.93
20%HF	745.93	480.01 (5th)	2.66	2.03	0.63	−5.21/−3.13
25%HF	640.23	431.65 (5th)	2.94	2.14	0.80	−5.79/−3.33
30%HF	559.65	391.41 (5th)	3.24	2.25	0.99	−6.39/−3.52
CB	404.22	356.02(4th)	3.36	2.61	0.75	−6.50/−1.92
Experimental emission wavelength: 624 nm						

state (with the lowest energy and nonzero oscillator strength) optimized geometry. For DMAC-DPS, we can see that 30% HF exchange would provide the best fit to the experimental results for the emission spectra wavelength (∼460 nm) measured at room temperature.[19] For DMAC-BP, our calculations suggest that 20% HF exchange can give the best fit to the experimental emission wavelength (∼516 nm).[20] Moreover, for the red-light-emitting DMAC-DCPP, 10% HF can give very good agreement with the experiments (∼624 nm).[21] For all the calculations of these three molecules with the percentages of HF exchange aforementioned, the singlet–triplet splittings are on the order of 0.1 eV (0.30 eV for DMAC-DPS, −0.34 eV for DMAC-BP, and −0.75 eV for DMAC-DCPP, corresponding to the optimal HF percentages), which is consistent with the previous experimental findings for TADF molecules.[9] Here, we can see the HOMO–LUMO gap, which will increase as we enlarge the proportion of HF exchange. The HF percentages have a larger influence on the HOMO energies than the LUMO, suggesting the importance of the HF exchange for the ionization potential.

Based on our calculations for DMAC-BP and DMAC-DCPP, we can also see the sign change of the singlet–triplet gaps, from positive (the normal gap) to negative (the inverted gap). For the majority of closed-shell molecules, the singlet–triplet gap is positive due to the direct exchange interaction (favoring the triplet state). The inverted gap found here could be due to two reasons. One is that the optimized geometry is for the triplet state, in which the excited singlet state could have a higher energy. The other is that in this triplet state geometry, the super-exchange mechanism could be more dominant due to the Coulomb repulsion energy and delocalized molecular orbitals than the direct exchange, thus leading to an inverted gap (an antiferromagnetic ground

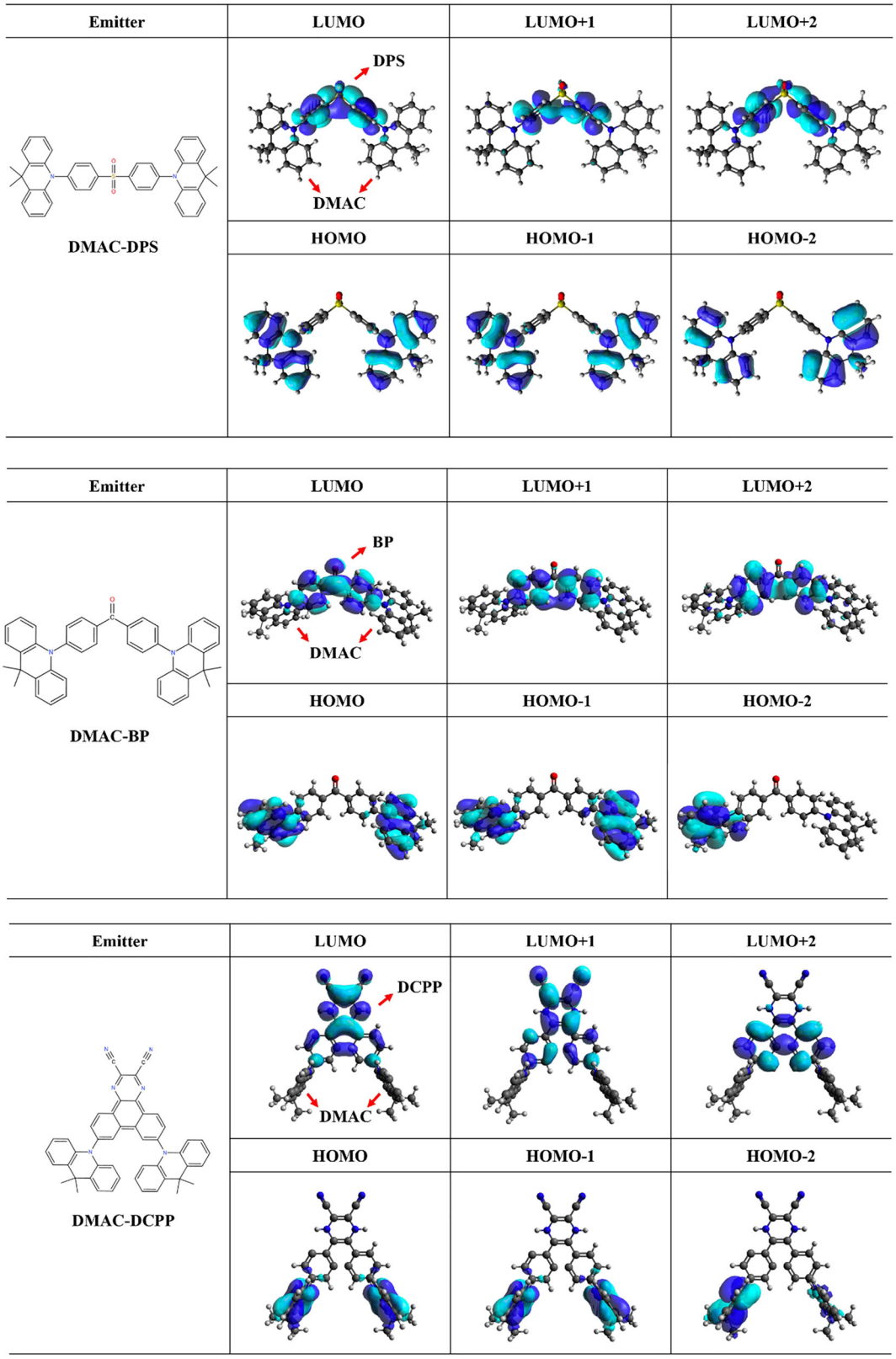

FIGURE 3 The molecular orbitals near the Fermi level (HOMO − 2 to LUMO + 2) for DMAC-DPS, DMAC-BP, and DMAC-DCPP. C is in gray, O in red, and H in white. For the molecular orbitals presented here, positive sign is in blue, negative in cyan

state).[40] The inverted gap has recently been attributed to the double excitation lowering the energy of the singlet excited state,[8] which is closely related to the doubly occupied intermediate state in the concept of super exchange.[40] In addition, we have also computed the singlet–triplet gaps at the optimized singlet ground state (not shown here), which are much smaller than those based on the triplet state. Recently, the inverted singlet–triplet gaps have been studied extensively because this would make the conversion from triplet to singlet more convenient than the conventional positive gap. This feature for DMAC-BP and DMAC-DCPP will facilitate the design of more efficient TADF OLED molecules. Moreover, the lifetime of the triplet state is important for the efficiency of the TADF molecules. The longer triplet lifetime implies the molecule has more chance to relax to the triplet-state geometry, thus improving the conversion rate from the triplet to the singlet. By contrast, the DMAC-DPS molecule has a robust normal gap, which could be due to the smaller difference between the optimized singlet and triplet geometries.

We have also calculated the electronic structures of these molecules by using the long-range-corrected hybrid-exchange DFT (CAM-B3LYP).[31] We have found that the absorption wavelength computed by CAM-B3LYP is better than B3LYP, whereas the emission spectra are not improved, as shown in the Tables 2–4. This could be due to the combination of the 20% HF and the long-range corrections applied, which will further localize the orbitals. The comparison between the calculations with and without long-range corrections suggests that we might not only need to correct the exchange functional but also use the double hybrid-exchange functional[41] to further improve the electronic correlations in the future study.

In Figure 3, we have shown the orbitals near the Fermi level, ranging from the HOMO − 2 to the LUMO + 2. For all the HOMO and LUMO orbitals, we can see that the HOMO orbitals are even in parity, whereas the LUMO orbitals are odd in parity. The HOMO orbitals are mainly distributed on the donors (DMAC molecules), whereas the LUMO orbitals are on the acceptors (DPS, BP, and DCPP molecules). All the occupied (unoccupied) orbitals shown here are on the donors (acceptors). This further confirms that all the molecules considered here are good candidates for OLED. The related excited states for the absorptions and emissions will be related to the HOMO–LUMO transitions, which are characterized by the charge-transfer process between the donors on the wings to the acceptors in the center. As we can see from the Tables 2–4, the HOMO–LUMO levels can be tuned by choosing different molecules for the acceptors, which provides an effective method to design molecules for different colors.

Because the energy level of HOMO of TADF molecules is determined by the donors' ability to donate electrons, the HOMO energy levels of the three molecules with the same donor are relatively close, between −6 and −4 eV (calculated at B3LYP/6-31G* level). The LUMO energy level is determined by the ability of electron acceptors. Therefore, the HOMO–LUMO energy level of the molecule can be adjusted by changing different acceptor molecules. The lower the LUMO level of the acceptor molecule, the smaller the energy level difference between HOMO and LUMO, and the longer the wavelength emitted by the molecule. In addition, smaller HOMO–LUMO gap implies the charge transfer between donor and acceptor would be easier, thus facilitating the overall device performance. Based on our calculations, the HOMO–LUMO gaps of DMAC-DPS, DMAC-DCPP, and DMAC-BP are ∼3.5, ∼3.0, and ∼2.5 eV, respectively. Therefore, the charge transfer would be eased for DMAC molecules with longer wavelength optical excitations. In this way, the emission color of the TADF molecule can be adjusted efficiently. At present, red molecules with high performance are relatively rare in TADF material research fields, which hinders the full-color display of OLEDs based on TADF materials.[42,43] Therefore, designing new red-emitting TADF materials is currently a hot research topic.

In order to design a TADF molecule with red-color light emission, we have chosen enaminone difluoroboron complexes (BFs) as the acceptor molecule, with LUMO energy level (−2.72 eV) which is similar to that of DCPP molecules and designed a new molecule called DMAC-BF connecting a central BF acceptor and two DMAC donors, as shown in Figure 2.

Similar to the previous three molecules, the LUMO of the DMAC-BF molecule is distributed on the acceptor unit in the center of the molecule. However, unlike the previous molecules, the HOMO of DMAC-BF is not symmetrically distributed. HOMO and HOMO − 1 are distributed on the two donors, respectively, as shown in Figure 4. This might be due to the fact that the two donors are too far apart by the three linearly connected benzene ring structures in the middle.

As the HF% in the functional increases, the calculated ΔE_{ST} value also becomes larger, but still on the order of 0.1 eV (except the CAM-B3LYP). The first active excited state of DMAC-BF molecule is the second excited state. Although the calculated emission wavelengths under different HF exchanges are different, the wavelengths are concentrated in the range of red light. According to the previous results, the optimal HF% for molecules with

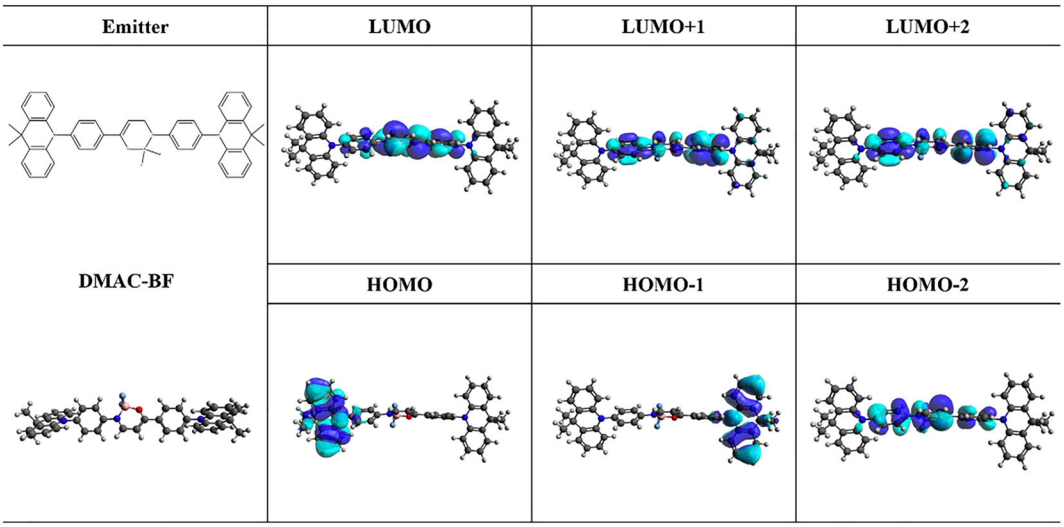

FIGURE 4 The molecular orbitals near the Fermi level (HOMO − 2 to LUMO + 2) for DMAC-BF

TABLE 5 Calculated results of DMAC-BF

	λ_{abs} (nm)	λ_{em} (nm)	S1 energy (eV)	T1 energy (eV)	ΔE_{ST} (eV)	HOMO/LUMO (eV)
15%HF	708.89	894.21 (2nd)	1.42	1.54	−0.12	−4.41/−2.38
20%HF	620.37	741.94 (2nd)	1.64	1.57	0.07	−5.01/−2.57
25%HF	550.14	630.71 (2nd)	1.86	1.55	0.31	−5.61/−2.77
30%HF	493.21	546.29 (2nd)	2.06	1.54	0.51	−6.23/−2.96
CB	378.67	332.23(2nd)	2.56	1.55	1.01	−6.33/−1.33

longer emission wavelengths is smaller, so we can guess that the most suitable HF% for DMAC-BF may be between 10% and 20%. In other words, its emission wavelength may be between 740 and 890 nm. Compared with the previous experiments for BF molecules (with one DMAC molecule), the emission spectra have not change significantly, which might be due to the weak interaction between acceptor and donor parts.

As shown in Table 5, the emission wavelengths and the singlet–triplet splittings for DMAC-BF (on the order of 0.1 eV) suggest that the DMAC-BF molecules are very suitable for working as TADF OLED molecules. Also, the computed emitted light wavelength with 15% HF indicates that the molecule has a very good potential for red-color TADF molecule. In addition, we can also see the inverted singlet–triplet gap from DMAC-BF calculation, which has been discussed in the previous sections. The CAM-B3LYP calculations show the similar trend as the other molecules aforementioned.

As shown in Figure 4, we can see the similar features for the orbitals near the HOMO. The LUMO is dominant at the acceptor (BF), whereas the HOMO at the donor (DMAC), suggesting DMAC-BF is also a good candidate for TADF charge-transfer molecules. The optical transitions for the red-color light emission would involve these molecular orbitals, thus having a charge-transfer characteristic. The singlet–triplet splitting also originates from the interaction between the HOMO and LUMO, which could be related to the super-exchange mechanism.

4 | CONCLUSIONS

In this paper, we have performed the first-principles calculations based on hybrid-exchange density functional with and without long-range corrections for four TADF molecules, DMAC-DPS, DMAC-BP, DMAC-DCPP, and DMAC-BF, to understand their optical emission and absorption spectra. We found that different percentages of HF exchange can be used in the hybrid-exchange density functional to obtain the consistent emission wavelength, as compared with the experimental results. The HF percentages for DMAC-DPS, DMAC-BP, DMAC-DCPP, and DMAC-BF are 30%, 20%, 10%, and 15%, respectively. Among these, only DMAC-BP molecule has the same percentage as the standard B3LYP functional. For our newly designed DMAC-BF molecule, we found

this is a potential candidate for red-color light emission. This proposed molecular structure can be used to compare with the existing TADF molecule with a red-color light emission. Our CAM-B3LYP calculations can provide a good estimate for the absorption spectra. However, we can see that we need use different percentages for these three molecules such that the agreement with the experimental results can be reached. This suggests that the further improvement to the exchange-correlation functional is needed for a proper description of both the absorption and emission spectra, which will be investigated in more details in the future. From the analysis of the excited-state wave functions, we can see the optical transition related to emission and absorption is dominated by the charge transfer between donor and acceptor moieties in a π-conjugated molecular plane. Most of the singlet–triplet splittings computed here are on the order of 0.1 eV, which is consistent with the previous related work. We have also found the inverted singlet–triplet gap for DMAC-BP, DMAC-DCPP, and DMAC-BF, which could facilitate the conversion from triplet to singlet, thus improving the performance of the TADF molecules. Moreover, in the future, we would also like to study the effects of the dispersion forces and solvent on the optical spectra of the TADF molecules.

ACKNOWLEDGEMENT

The authors thank the UCL Research Computing Team for the technical support. W.W. would like to acknowledge the funding support from the EU Marketplace project 545083.

DATA AVAILABILITY STATEMENT

The data that support the findings of this study are available from the corresponding author upon reasonable request.

ORCID

Yuting Wang https://orcid.org/0000-0003-2888-2466
Wei Wu https://orcid.org/0000-0003-2843-5113

REFERENCES

[1] H.-W. Chen, J.-H. Lee, B.-Y. Lin, S. Chen, S.-T. Wu, *Light: Sci. Appl* **2018**, *7*, 17168. https://doi.org/10.1038/lsa.2017.168
[2] Y. Huang, E.-L. Hsiang, M.-Y. Deng, S.-T. Wu, *Light: Sci. Appl* **2020**, *9*, 105. https://doi.org/10.1038/s41377-020-0341-9
[3] B. Geffroy, P. le Roy, C. Prat, *Polym. Int.* **2006**, *55*, 572. https://doi.org/10.1002/pi.1974
[4] C. Adachi, *Jpn. J. Appl. Phys.* **2014**, *53*, 060101. https://doi.org/10.7567/JJAP.53.060101
[5] J. H. Burroughes, D. D. C. Bradley, A. R. Brown, R. N. Marks, K. Mackay, R. H. Friend, P. L. Burns, A. B. Holmes, *Nature* **1990**, *347*, 539. https://doi.org/10.1038/347539a0
[6] M. A. Baldo, D. F. O'Brien, Y. You, A. Shoustikov, S. Sibley, M. E. Thompson, S. R. Forrest, *Nature* **1998**, *395*, 151. https://doi.org/10.1038/25954
[7] H. Uoyama, K. Goushi, K. Shizu, H. Nomura, C. Adachi, *Nature* **2012**, *492*, 234. https://doi.org/10.1038/nature11687
[8] P. de Silva, *J. Phys. Chem. Lett.* **2019**, *10*, 5674. https://doi.org/10.1021/acs.jpclett.9b02333
[9] Y. Tao, K. Yuan, T. Chen, P. Xu, H. Li, R. Chen, C. Zheng, L. Zhang, W. Huang, *Adv. Mater.* **2014**, *26*, 7931. https://doi.org/10.1002/adma.201402532
[10] W.-L. Tsai, M.-H. Huang, W.-K. Lee, Y.-J. Hsu, K.-C. Pan, Y.-H. Huang, H.-C. Ting, M. Sarma, Y.-Y. Ho, H.-C. Hu, C.-C. Chen, M.-T. Lee, K.-T. Wong, C.-C. Wu, *Chem. Commun.* **2015**, *51*, 13662. https://doi.org/10.1039/C5CC05022G
[11] W. Li, B. Li, X. Cai, L. Gan, Z. Xu, W. Li, K. Liu, D. Chen, S.-J. Su, *Angew. Chem. Int. Ed.* **2019**, *58*, 11301. https://doi.org/10.1002/anie.201904272
[12] D. H. Ahn, S. W. Kim, H. Lee, I. J. Ko, D. Karthik, J. Y. Lee, J. H. Kwon, *Nat. Photonics* **2019**, *13*, 540. https://doi.org/10.1038/s41566-019-0415-5
[13] Q. Wei, Z. Ge, B. Voit, *Macromol. Rapid Commun.* **2019**, *40*, 1800570. https://doi.org/10.1002/marc.201800570
[14] B. Wex, B. R. Kaafarani, *J. Mater. Chem. C* **2017**, *5*, 8622. https://doi.org/10.1039/C7TC02156A
[15] A. Stoïanov, C. Gourlaouen, S. Vela, C. Daniel, *J. Phys. Chem. A* **2018**, *122*, 1413. https://doi.org/10.1021/acs.jpca.7b11793
[16] H. Tanaka, K. Shizu, H. Miyazaki, C. Adachi, *Chem. Commun.* **2012**, *48*, 11392. https://doi.org/10.1039/c2cc36237f
[17] Y. Kang, L. Zhao, J. Leng, *Chem. Phys. Lett.* **2018**, *698*, 187. https://doi.org/10.1016/j.cplett.2018.03.017
[18] S. Huang, Q. Zhang, Y. Shiota, T. Nakagawa, K. Kuwabara, K. Yoshizawa, C. Adachi, *J. Chem. Theory Comput.* **2013**, *9*, 3872. https://doi.org/10.1021/ct400415r
[19] Q. Zhang, B. Li, S. Huang, H. Nomura, H. Tanaka, C. Adachi, *Nat. Photonics* **2014**, *8*, 326. https://doi.org/10.1038/nphoton.2014.12
[20] X. Jiang, H. Lin, C. Xue, G. Zhang, W. Jiang, G. Xing, *J. Mater. Sci. Mater. Electron.* **2020**, *31*, 19136. https://doi.org/10.1007/s10854-020-04450-z
[21] S. Wang, Z. Cheng, X. Song, X. Yan, K. Ye, Y. Liu, G. Yang, Y. Wang, *ACS Appl. Mater. Interfaces* **2017**, *9*, 9892. https://doi.org/10.1021/acsami.6b14796
[22] H. Li, H. Shu, X. Wang, X. Wu, H. Tian, H. Tong, L. Wang, *Dyes Pigm.* **2021**, *184*, 108810. https://doi.org/10.1016/j.dyepig.2020.108810
[23] Q. Zhang, D. Tsang, H. Kuwabara, Y. Hatae, B. Li, T. Takahashi, S. Y. Lee, T. Yasuda, C. Adachi, *Adv. Mater.* **2015**, *27*, 2096. https://doi.org/10.1002/adma.201405474
[24] M. Haroon, M. R. S. A. Janjua, *Energy Fuel* **2021**, *35*, 12461. https://doi.org/10.1021/acs.energyfuels.1c01726
[25] M. Haroon, M. R. S. A. Janjua, *J. Comput. Electron.* **2022**, *21*, 40. https://doi.org/10.1007/s10825-021-01838-w
[26] M. Haroon, M. R. S. A. Janjua, *J. Phys. Org. Chem.* **2022**, *n/a*, e4353.
[27] M. Haroon, A. A. Al-Saadi, M. R. S. A. Janjua, *J. Phys. Org. Chem.* **2022**, *35*, e4314. https://doi.org/10.1002/poc.4314
[28] M. Haroon, M. Khalid, Z. Shafiq, M. U. Khan, M. R. S. A. Janjua, *Mater. Today Commun.* **2021**, *27*, 102485. https://doi.org/10.1016/j.mtcomm.2021.102485

[29] A. Saeki, K. Kranthiraja, *Jpn. J. Appl. Phys.* **2019**, *59*, SD0801. https://doi.org/10.7567/1347-4065/ab4f39

[30] Y. Im, M. Kim, Y. J. Cho, J.-A. Seo, K. S. Yook, J. Y. Lee, *Chem. Mater.* **2017**, *29*, 1946. https://doi.org/10.1021/acs.chemmater.6b05324

[31] T. Yanai, D. P. Tew, N. C. Handy, *Chem. Phys. Lett.* **2004**, *393*, 51. https://doi.org/10.1016/j.cplett.2004.06.011

[32] R. G. Parr, *Annu. Rev. Phys. Chem.* **1983**, *34*, 631. https://doi.org/10.1146/annurev.pc.34.100183.003215

[33] V. Peuckert, *J. Phys C: Solid State Phys.* **1978**, *11*, 4945. https://doi.org/10.1088/0022-3719/11/24/023

[34] R. Li, J. Zheng, D. G. Truhlar, *Phys. Chem. Chem. Phys.* **2010**, *12*, 12697. https://doi.org/10.1039/c0cp00549e

[35] T. Stein, L. Kronik, R. Baer, *J. Am. Chem. Soc.* **2009**, *131*, 2818. https://doi.org/10.1021/ja8087482

[36] T. Zou, X. Wang, H. Ju, Q. Wu, T. Guo, W. Wu, H. Wang, *J. Mater. Chem. C* **2018**, *6*, 1495. https://doi.org/10.1039/C7TC04663D

[37] G. W. Trucks, H. B. Schlegel, G. E. Scuseria, J. R. C. M. A. Robb, G. Scalmani, V. Barone, B. Mennucci, H. N. G. A. Petersson, M. Caricato, X. Li, H. P. Hratchian, J. B. A. F. Izmaylov, G. Zheng, J. L. Sonnenberg, M. Hada, K. T. M. Ehara, R. Fukuda, J. Hasegawa, M. Ishida, T. Nakajima, O. K. Y. Honda, H. Nakai, T. Vreven, J. A. Montgomery Jr., F. O. J. E. Peralta, M. Bearpark, J. J. Heyd, E. Brothers, V. N. S. K. N. Kudin, T. Keith, R. Kobayashi, J. Normand, A. R. K. Raghavachari, J. C. Burant, S. S. Iyengar, J. Tomasi, N. R. M. Cossi, J. M. Millam, M. Klene, J. E. Knox, J. B. Cross, C. A. V. Bakken, J. Jaramillo, R. Gomperts, R. E. Stratmann, A. J. A. O. Yazyev, R. Cammi, C. Pomelli, J. W. Ochterski, K. M. R. L. Martin, V. G. Zakrzewski, G. A. Voth, J. J. D. P. Salvador, S. Dapprich, A. D. Daniels, J. B. F. O. Farkas, J. V. Ortiz, J. Cioslowski, *Gaussian 09, M. J. F. Revision D.01*, D. J. Fox, Inc, Wallingford CT **2013**.

[38] L. E. de Sousa, P. de Silva, *J. Chem. Theory Comput.* **2021**, *17*, 5816. https://doi.org/10.1021/acs.jctc.1c00476

[39] M. D. Hanwell, D. E. Curtis, D. C. Lonie, T. Vandermeersch, E. Zurek, G. R. Hutchison, *J. Chem.* **2012**, *4*, 17. https://doi.org/10.1186/1758-2946-4-17

[40] P. W. Anderson, *Phys. Rev.* **1950**, *79*, 350. https://doi.org/10.1103/PhysRev.79.350

[41] K. Sharkas, J. Toulouse, A. Savin, *J. Chem. Phys.* **2011**, *134*, 064113. https://doi.org/10.1063/1.3544215

[42] J.-X. Chen, K. Wang, C.-J. Zheng, M. Zhang, Y.-Z. Shi, S.-L. Tao, H. Lin, W. Liu, W.-W. Tao, X.-M. Ou, X.-H. Zhang, *Adv. Sci.* **2018**, *5*, 1800436. https://doi.org/10.1002/advs.201800436

[43] X. Gong, P. Li, Y.-H. Huang, C.-Y. Wang, C.-H. Lu, W.-K. Lee, C. Zhong, Z. Chen, W. Ning, C.-C. Wu, S. Gong, C. Yang, *Adv. Funct. Mater.* **2020**, *30*, 1908839. https://doi.org/10.1002/adfm.201908839

[44] R. Dhali, D. K. A. P. Huu, F. Bertocchi, C. Sissa, F. Terenziani, A. Painelli, *Phys. Chem. Chem. Phys.* **2021**, *23*, 378. https://doi.org/10.1039/D0CP05982J

How to cite this article: Y. Wang, W. Wu, K. L. Choy, *J Phys Org Chem* **2022**, e4386. https://doi.org/10.1002/poc.4386